

SLAM with Joint Sensor Bias Estimation: Closed Form Solutions on Observability, Error Bounds and Convergence Rates

L.D.L. Perera, W.S. Wijesoma and M.D. Adams

Abstract— Notable problems in Simultaneous Localization and Mapping (SLAM) are caused by biases and drifts in both exteroceptive and proprioceptive sensors. The impacts of sensor biases include inconsistent map estimates and inaccurate localization. Unlike Map Aided Localisation with Joint Sensor Bias Estimation (MAL-JSBE), SLAM with Joint Sensor Bias Estimation (SLAM-JSBE) is more complex as it encompasses a state space, which increases with the discovery of new landmarks and the inherent map to vehicle correlations. The properties such as observability, error bounds and convergence rates of SLAM-JSBE using an augmented estimation theoretic, state space approach, are investigated here. SLAM-JSBE experiments, which adhere to the derived constraints, are demonstrated using a low cost inertial navigation sensor suite.

Index Terms— bias estimation, mapping, Robot localization

NOMENCLATURE

MAL	Map Aided Localization.
SLAM	Simultaneous Localization and Mapping.
JSBE	Joint Sensor Bias Estimation.
MAL-JSBE	Map Aided Localization with Joint Sensor Bias Estimation.
SLAM-JSBE	Simultaneous Localization and Mapping with Joint Sensor Bias Estimation.
1D	Single degree of freedom.
2D	2 degrees of freedom.
IMU	Inertial Measurement Unit
LMS	Laser Measurement System
I_n	Identity matrix of size $n \times n$
$\mathbf{0}_n$	Square matrix of size $n \times n$ with all zero elements
$\lambda_{m \times n}$	Matrix of size $m \times n$ with every element is λ

I. INTRODUCTION

MAL or map aided localization is the process of a vehicle localizing itself at all times, assuming that

Manuscript received on 2 June, 2008, revised on 15 December 2008. Manuscript received in final form on 15 June 2009. Recommended by Associate Editor Jay Lee. The first author acknowledges the support of the Rio-Tinto Centre for Mine Automation and the ARC Centre of Excellence program funded by the Australian Research Council (ARC) and the New South Wales Government.

The first author is with the Australian Centre for Field Robotics, The University of Sydney, Australia. {email: l.perera@acfr.usyd.edu.au}

The second and third authors are with Nanyang Technological University, Singapore.

prior environmental knowledge is available. In [15], the authors provided an extensive theoretical analyses and important results of the problem of Map Aided Localization with Joint Sensor Bias Estimation (MAL-JSBE).

As opposed to MAL, SLAM does not presuppose the availability of an a priori map, but with the aid of the robot's onboard exteroceptive and proprioceptive sensors, attempts to incrementally build a feature map of the robot's environment and use this to localize the robot. Works [4], [16] and [17] provide rigorous analyses of the convergence of uncertainties, rates of convergence and observability properties of the estimation theoretic, Extended Kalman Filter (EKF) based standard SLAM algorithm.

Even though, SLAM has stimulated considerable interest in the mobile robotics community, as evident from the plethora of SLAM formulations, algorithms and implementations reported in the literature, the effects and implications of exteroceptive and proprioceptive sensor biases on SLAM have been largely ignored. The propagation of sensor errors (both systematic and random) in SLAM often results in inaccurate localization estimates (as in MAL) as well as inconsistent maps. It is noted in [1] that as more features are added to the map, the inherent map-to-vehicle correlations results in the spread of bias errors throughout the map causing the EKF-SLAM filter to diverge. Time varying biases arising from modeling errors, sensor biases and imperfect calibrations also contribute to map divergence even if the sensors are accurately initialized or calibrated prior to their use. The cumulative effects of sensor biases and modeling offsets often cause significant problems in large-scale SLAM implementations. Furthermore, it is also observed in [1] that bias errors significantly impair tracking accuracy and data association in the context of the SLAM problem. In summary, it can be conjectured that the negative impacts of bias errors on SLAM are significant and more adverse than on MAL. In this paper we extend our work on MAL-JSBE [15] to SLAM-JSBE, verify the results through simulations and experimental results, and compare the theoretical results obtained with those of [4], [15], [16] and [17].

Works [2], [3], [13] and [15] review the various sensor bias estimation techniques and their merits and demerits. Although, offline calibration of a sensor can minimize the ill effects of its bias, the process results in longer set-up and processing times. Moreover, these calibrations are not effective in the long run if the biases are subject to frequent changes and drifts. This motivates one to model and on-line estimate sensors' bias parameters jointly with the vehicle and map states using an augmented state space approach [5]. In [6], Okkello and Challa describe a radar bias estimation, joint registration and track-to-track fusion method based on measurements collected from geographically separated radar trackers, whose locations are fixed. In a similar vain, we use the augmented state vector method for the joint estimation of sensor biases, vehicle localization and map estimates

using an estimation theoretic framework.

Section II, discusses the properties of the 1D SLAM-JSBE problem. Section III, investigates the properties of the 2D SLAM-JSBE problem. Section IV discusses IMU aided SLAM-JSBE and provides experimental results utilizing an IMU and other sensors. Section V concludes the work.

II. BIAS CORRECTION IN THE SINGLE DEGREE OF FREEDOM SLAM PROBLEM

A. Problem Formulation

To better appreciate the effects of sensor biases and it's analysis in the context of the SLAM problem, we start off with the simple 1D SLAM problem. 1D SLAM problem ([16]) is a linear estimation problem. Let the location of the vehicle and vehicle's proprioceptive and exteroceptive sensors' biases at time k be $x_v(k)$, $u_b(k)$ and $s_b(k)$ respectively. The augmented process model (incorporating the unknown sensor bias parameters) for 1D SLAM-JSBE and the corresponding measurement model, when observing n landmarks are

$$\mathbf{X}(k) = \mathbf{F}\mathbf{X}(k-1) + \begin{bmatrix} u(k-1) \\ \mathbf{0}_{(n+2) \times 1} \end{bmatrix} + \begin{bmatrix} v(k-1) \\ \mathbf{0}_{(n+2) \times 1} \end{bmatrix} \quad (1)$$

$$\mathbf{z}(k) = \mathbf{H}\mathbf{X}(k) + \mathbf{w}(k) \quad (2)$$

where $\mathbf{F} = \begin{bmatrix} 1 & 1 & \mathbf{0}_{1 \times (n+1)} \\ 0 & 1 & \mathbf{0}_{1 \times (n+1)} \\ \mathbf{0}_{(n+1) \times 1} & \mathbf{0}_{(n+1) \times 1} & \mathbf{I}_{n+1} \end{bmatrix}$, $\mathbf{H} = \begin{bmatrix} -1_{n \times 1} & \mathbf{0}_{n \times 1} & \mathbf{1}_{n \times 1} & \mathbf{I}_n \end{bmatrix}$

and $\mathbf{X}^T(k) = [x_v(k) \ u_b(k) \ s_b(k) \ \mathbf{m}^T(k)]^T$. The proprioceptive sensor input is $u(k-1)$, the proprioceptive sensor input noise is $v(k-1) \sim N(0, q^2)$, the measurement noise is $\mathbf{w}(k) \sim N(\mathbf{0}_{n \times 1}, r^2 \mathbf{I}_n)$. q^2 and r^2 are the variances of $v(k)$ and the exteroceptive measurement noise when observing one landmark. $\mathbf{m}(k)$ is the n landmark map state of 1D landmark locations.

B. Observability Conditions in 1D

Observability is one of the important requirements as far as the choice of a process model and an observation model for an estimation theoretic algorithm is concerned. With the usual notation (1) and (2) in terms of linearized error states are as follows.

$$\tilde{\mathbf{X}}(k) = \mathbf{F}\tilde{\mathbf{X}}(k-1) + \mathbf{B} \begin{bmatrix} v(k-1) & \mathbf{0}_{1 \times (n+2)} & \mathbf{w}^T(k) \end{bmatrix}^T \quad (3)$$

$$\tilde{\mathbf{z}}(k) = \mathbf{H}\tilde{\mathbf{X}}(k) + \mathbf{H}_w \begin{bmatrix} v(k-1) & \mathbf{0}_{1 \times (n+2)} & \mathbf{w}^T(k) \end{bmatrix}^T \quad (4)$$

$\tilde{\mathbf{X}}(k)$ and $\tilde{\mathbf{z}}(k)$ denote the error of actual and estimated states of $\mathbf{X}(k)$ and $\mathbf{z}(k)$ respectively. Observability and controllability Grammians \mathbf{G}_O and \mathbf{G}_C . for linear time invariant systems such as (3) and (4) are as follows

$$\mathbf{G}_O = \left[(\mathbf{H}\mathbf{F})^T \ (\mathbf{H}\mathbf{F}^2)^T \ \dots \ (\mathbf{H}\mathbf{F}^i)^T \right]^T \quad (5)$$

$$\mathbf{G}_C = \left[\mathbf{B} \ \mathbf{F}\mathbf{B} \ \mathbf{F}^2\mathbf{B} \ \dots \ \mathbf{F}^{i-1}\mathbf{B} \right] \quad (6)$$

where i is the dimension of the state vector $\tilde{\mathbf{X}}(k)$. The

system is controllable if \mathbf{G}_C has a rank of i and observable if \mathbf{G}_O has a rank of i . Now $\text{Image}(\mathbf{G}_C)$ and $\text{Image}(\mathbf{G}_O^T)$ (where $\text{Image}(\mathbf{X})$ denotes a basis of the image of the vector space of \mathbf{X}) can be obtained from (3)-(6). Hence from the $\text{Image}(\mathbf{G}_O^T)$ it follows that the rank of the observability Grammian is $n+1$. Thus, the 1D SLAM-JSBE is partially observable as in the case of 1D MAL-JSBE [15] and 1D SLAM [17]. This partial observability can be expressed in terms of an angle ψ which is the angle between the controllable and observable subspaces. It is important to note that assuming a known initial state does not affect the observability results, since history of measurements are not uniquely related to the initial state in an unobservable system.

Result 1: The angle, ψ between the controllable and observable subspaces in 1D SLAM-JSBE is a function of the number of landmarks in the map only and is given by

$$\psi = \cos^{-1} \left(\frac{1}{\sqrt{n/(2n+1)}} \right) \quad (7)$$

It may be noted that ψ is a monotonically decreasing function of n , and as such as the number of observed landmarks increase, the observable subspace gets closer to the controllable region of the state space. However, ψ cannot be reduced below $\pi/4$.

As emphasized in [10], another important scenario is when the proprioceptive sensor bias exhibits random walk behavior which is often present in common rate sensors. In such a scenario, $\mathbf{X}(k)$, \mathbf{F} , \mathbf{H} and $\mathbf{z}(k)$ take the same form as in (3) and (4), however the linearized error state is now,

$$\tilde{\mathbf{X}}(k) = \mathbf{F}\tilde{\mathbf{X}}(k-1) + \tilde{\mathbf{B}} \begin{bmatrix} v(k-1) & v_b(k-1) & \mathbf{0}_{1 \times (n+1)} & \mathbf{w}^T(k) \end{bmatrix}^T \quad (8)$$

where, the noise $v_b(k)$ in proprioceptive sensor bias term is zero mean Gaussian. As before for this system we can obtain the $\text{Image}(\mathbf{G}_O^T)$ and $\text{Image}(\mathbf{G}_C)$ and hence show that the rank of \mathbf{G}_O^T is $n+1$, and thus is rank deficient by 2.

The angle between any two subspaces \mathbf{F} and \mathbf{G} with \mathbf{Q}_F and \mathbf{Q}_G as orthonormal bases is given by the inverse cosine of the smallest singular value of $\mathbf{Q}_F^T \mathbf{Q}_G$. Using this result it is possible to verify that in this case too, the angle between the controllable and observable subspaces, ψ resembles the expression (7). One way to achieve full observability of the 1D SLAM is to incorporate a known landmark observation and the absolute position information of the vehicle as measured by an absolute position measurement sensor system, such as GPS, in to the measurement vector. The observation matrix \mathbf{H} of 1D SLAM-JSBE when observing n unknown landmarks, one known landmark and the absolute vehicle position would then be

$$\mathbf{H} = \begin{bmatrix} -1_{n \times 1} & \mathbf{0}_{n \times 1} & \mathbf{1}_{n \times 1} & \mathbf{I}_n \\ -1 & 0 & 1 & \mathbf{0}_{1 \times n} \\ 1 & 0 & 0 & \mathbf{0}_{1 \times n} \end{bmatrix} \quad (9)$$

In this instance it can be easily verified that \mathbf{G}_O^T is rank $n+3$, and is equal to the dimension of the full state vector.

Hence, the system is now fully observable and $\text{Image}(\mathbf{G}_C) = \begin{bmatrix} 1 & \mathbf{0}_{1 \times (n+3)} \end{bmatrix}^T$. Consequently, the angle between the controllable and observable subspaces is now zero.

C. Rates of Convergence of Uncertainties in 1D

The rate of convergence of uncertainties is one of the key issues invaluable in evaluating the performance of an estimation algorithm in terms of speed. Consider the continuous time equivalent of the 1D SLAM-JSBE state (1) and (2) incorporating only one unknown landmark. It is assumed that $\mathbf{w}(t)$ corresponding to $\mathbf{w}(k)$ in (2) is $\mathbf{w}(t) \sim N(\mathbf{0}_{3 \times 1}, \mathbf{R})$ $\mathbf{R} = \text{diag}(r^2, r_e^2, r_e^2)$ is the covariance matrix of $\mathbf{w}(t)$, and r^2 and r_e^2 are the variances of the exteroceptive and absolute sensor measurement noises respectively. \mathbf{H} is given by (9) ($n=1$). Suppose that $\mathbf{P}(t)$ is the covariance matrix of $\mathbf{X}(t)$. Thus, $\mathbf{P}(t)$ can be obtained by the solution of the continuous time Riccati equation

$$\dot{\mathbf{P}}(t) = \mathbf{F}\mathbf{P}(t) + \mathbf{P}(t)\mathbf{F}^T + \mathbf{G}\mathbf{Q}\mathbf{G}^T - \mathbf{P}(t)\mathbf{H}^T\mathbf{R}^{-1}\mathbf{H}\mathbf{P}(t) \quad (10)$$

where $\mathbf{P}(0) = \text{diag}(0, \sigma_{bu}^2, \sigma_{bs}^2, \sigma_m^2)$. σ_{bu}^2 , σ_{bs}^2 and σ_m^2 denote the initial variances of proprioceptive and exteroceptive sensor biases and map consisting of the unknown landmark respectively. Except that of the vehicle position, solution to (10) (see [15] for the solution method) shows that all the steady state covariance terms, $\mathbf{P}(\infty)$, approach zero. As there is continuous noise injected into the vehicle motion model, in the form of process noise when the vehicle is moving, the vehicle position variance approaches q^2/α , where, $\alpha = (q/(rr_e))(2r_e^2 + r^2)^{0.5}$. This further shows that the error covariance terms of $\mathbf{X}(t)$, initially decay exponentially with a time constant of $1/\alpha$ and then converge asymptotically to the steady state covariance. Suppose that n_1 unknown landmark locations are estimated in the SLAM-JSBE state vector while observing n_2 known landmarks. Then if an absolute sensor measurement of the robot position is incorporated it follows that:

$$\alpha = (q/(rr_e))\sqrt{(n_1 + n_2)r_e^2 + r^2} \quad (11)$$

It is interesting to note that this convergence rate α is not affected by the biases or their initial uncertainties. When $r_e^2 \gg r^2$ (i.e. landmark based information dominates the absolute position sensor based information) this time constant (τ) can be expressed as:

$$\tau = (r/(q\sqrt{n_1 + n_2})) \quad (12)$$

Hence we can arrive at the following result.

Result 2: The smaller the ratio between the exteroceptive sensor noise and the process noise (proprioceptive sensor noise and the modeling uncertainty) or the larger the number of landmarks observed simultaneously (known, estimated or both), the faster will be the convergence of the state variances to their steady state values.

It is ascertained from (12) that the uncertainties of 1D SLAM-JSBE converge much faster than those of 1D MAL-JSBE [15].

III. BIAS CORRECTION IN THE TWO DEGREES OF FREEDOM SLAM PROBLEM

A. Problem Formulation

In the 2D (planar) SLAM problem, a vehicle traversing on a 2D plane incrementally builds a map $\mathbf{m}(k)$ of n landmarks situated on the same plane, whilst using this map to localize itself. Let the location of the vehicle on the plane be $\mathbf{x}_v(k) = [x(k) \ y(k) \ \theta(k)]^T$ where $x(k)$, $y(k)$ and $\theta(k)$ denote coordinates (mid point of the rear axel) and heading of the vehicle with respect to a global coordinate frame.

$\mathbf{m}(k) = [x_1(k) \ y_1(k) \dots x_n(k) \ y_n(k)]^T$ is the feature map where point feature position vectors $[x_i(k) \ y_i(k)]^T$ $i=1, 2, \dots, n$ are specified with respect to the same global coordinate frame. Let $\mathbf{u}(k)$ denote the proprioceptive sensor input; $\mathbf{v}(k) \sim N(\mathbf{0}, \mathbf{Q}_v(k))$ denote the modeling uncertainties having a covariance matrix of $\mathbf{Q}_v(k)$; $\mathbf{u}_b(k)$ denote the concatenated proprioceptive sensor biases and $\mathbf{s}_b(k)$ denote the concatenated exteroceptive sensor biases. The process and observation models of the 2D SLAM-JSBE problem are then

$$\mathbf{X}(k | k-1) = \begin{bmatrix} \mathbf{f}_v(\mathbf{x}_v(k-1), \mathbf{u}(k-1), \mathbf{u}_b(k)) \\ \mathbf{x}_b(k-1) \\ \mathbf{m}(k-1) \end{bmatrix} + \begin{bmatrix} \mathbf{v}(k-1) \\ \mathbf{v}_b(k-1) \\ \mathbf{0}_{2n} \end{bmatrix} \quad (13)$$

$$\mathbf{z}(k) = \mathbf{h}(\mathbf{x}_v(k), \mathbf{m}(k), \mathbf{s}_b(k)) + \mathbf{w}(k) \quad (14)$$

where $\mathbf{x}_b(k) = [\mathbf{u}_b^T(k) \ \mathbf{s}_b^T(k)]^T$, $\mathbf{X}(k) = [\mathbf{x}_v^T(k) \ \mathbf{x}_b^T(k) \ \mathbf{m}^T(k)]$, $\mathbf{v}_b(k)$ represents a temporally, uncorrelated noise sequence of the sensor biases, $\mathbf{w}(k)$ is the vector of observation noise, assumed Gaussian with zero mean and covariance $\mathbf{R}(k)$, $\mathbf{f}_v(\cdot)$ is a nonlinear function representing the robot motion model and $\mathbf{h}(\cdot)$ is the observation model of the exteroceptive sensors used by the robot.

B. Diminishing Uncertainty of Bias Estimates

SLAM-JSBE for the case of unknown, constant biases, using the linearized models of (13) and (14) can be summarized as follows. The process model is given by,

$$\mathbf{X}(k) = \mathbf{F}\mathbf{X}(k-1) + \begin{bmatrix} \mathbf{B}_v(\mathbf{u}(k-1)) \\ \mathbf{0}_{n_1 \times 1} \end{bmatrix} + \begin{bmatrix} \mathbf{v}(k) \\ \mathbf{0}_{n_1 \times 1} \end{bmatrix} \quad (15)$$

where \mathbf{B}_v is the transition matrix of the proprioceptive sensor measurements and $\mathbf{v}(k) \sim N(\mathbf{0}, \mathbf{Q}_v(k))$. The sensor bias state $\mathbf{x}_b(k)$, augmented state $\mathbf{X}(k)$ and observation noise $\mathbf{w}(k)$ are assumed to be of the same form and meaning as (13) and (14). n_1 is the total dimension of the bias states and map states. \mathbf{F} and \mathbf{F}_b are given by

$$\mathbf{F} = \begin{bmatrix} \mathbf{F}_b & | & \mathbf{0}_{bm} \\ \mathbf{0}_{bm}^T & | & \mathbf{I}_{mm} \end{bmatrix} \text{ and } \mathbf{F}_b = \begin{bmatrix} \mathbf{F}_v & \mathbf{B}_v & \mathbf{0}_{vs} \\ \mathbf{0}_{vu}^T & \mathbf{I}_{uu} & \mathbf{0}_{us} \\ \mathbf{0}_{vs}^T & \mathbf{0}_{us}^T & \mathbf{I}_{ss} \end{bmatrix} \quad (16)$$

where subscripts m denote the entire map state, v the vehicle

state, u the proprioceptive sensor bias vector and s the exteroceptive sensor bias vector. Matrices, \mathbf{I}_{ss} , \mathbf{I}_{uu} and \mathbf{I}_{mm} are identity matrices with dimensions $\dim(\mathbf{s}_b) \times \dim(\mathbf{s}_b)$, $\dim(\mathbf{u}_b) \times \dim(\mathbf{u}_b)$ and $\dim(\mathbf{m}) \times \dim(\mathbf{m})$ respectively. $\mathbf{0}_{vs}$, $\mathbf{0}_{vu}$ and $\mathbf{0}_{us}$ are null matrices having appropriate dimensions. The corresponding observation model is;

$$\mathbf{z}(k) = \mathbf{H}(k)\mathbf{X}(k) + \mathbf{w}(k) \quad (17)$$

where $\mathbf{H}(k) = \begin{bmatrix} -\mathbf{H}_v(k) & \mathbf{0}_{uu} & \mathbf{I}_{ss} & \mathbf{H}_m(k) \end{bmatrix}$. $-\mathbf{H}_v(k)$, $\mathbf{H}_m(k)$ and $\mathbf{0}_{uu}$ denote the parts of $\mathbf{H}(k)$ corresponding to vehicle states, map states and a null matrix of dimension $\dim(\mathbf{u}_b) \times \dim(\mathbf{u}_b)$. By investigating the above models (15)-(17), the following important result can be derived.

Result 3: The uncertainties in the estimates of the proprioceptive and exteroceptive sensor bias parameters diminish monotonically in an update of the SLAM algorithm (See Appendix for the proof).

Thus it can be conjectured that as the estimated environmental map state errors decrease, so do those of the proprioceptive and exteroceptive sensor bias errors.

C. Uncertainty Bounds

It is important to investigate whether the diminishing uncertainties of the bias error states will eventually reach a finite lower limit or zero. Suppose that \mathbf{P}_v denotes the initial vehicle covariance matrix, \mathbf{P}_m the initial map covariance matrix and \mathbf{P}_s the initial exteroceptive sensor bias covariance matrix of $\mathbf{P}_{ss}(k|k)$. Theoretical analysis yields the following Result 4.

Result 4: The uncertainties in the estimates of the exteroceptive sensor bias parameters in 2D SLAM-JSBE reach a lower bound as determined by the process and observation model error covariances.

For two special cases of SLAM-JSBE, these lower bounds can be derived in closed form as follows.

Case 1: The initial values of exteroceptive sensor biases are completely unknown. From (36) to (39) given in the Appendix, it follows that $\mathbf{P}_{ss}(k|k) = \mathbf{H}_m\mathbf{P}_m\mathbf{H}_m^T + \mathbf{H}_v\mathbf{P}_v\mathbf{H}_v^T$. Thus, the lower bound of the exteroceptive sensor bias terms is entirely determined by the initial covariance estimates of the vehicle (\mathbf{P}_v) and the unknown, or estimated, landmark (\mathbf{P}_m). According to [15], the lower bound ($\mathbf{H}_v\mathbf{P}_v\mathbf{H}_v^T$) of the exteroceptive sensor bias terms in MAL-JSBE is lower than the lower bound for SLAM-JSBE. This can be attributed to the fact that in the case of MAL, the information acquired is entirely utilized for vehicle localization and sensor bias estimation.

Case 2: The initial landmark position uncertainty is very large ($\mathbf{P}_m \rightarrow \infty$). Under these circumstances $\mathbf{P}_{ss}(k|k) = \mathbf{P}_s$ implying that the uncertainties of the exteroceptive sensor biases cannot be reduced by observing unknown landmarks from a stationary vehicle.

D. Observability in 2D SLAM-JSBE

The Result 4 suggests that 2D SLAM-JSBE is not fully

observable. If the above problem is fully observable $\mathbf{P}_{ss}(k|k)$ should approach zero or a value independent of the initial conditions. Although, it is difficult to ascertain the conditions that must be satisfied for full observability in non-linear, time varying systems, these conditions have been derived in [9], [14] and [15] under certain assumptions. In [9], [14] and [15] conditions for observability are derived through rank analysis of the observability matrices constructed from linearized Jacobians of the piecewise constant process and observation models. However, it is important to note that rank analysis provides necessary conditions and not sufficient conditions according to [9]. We use the technique described in [15] to analyze the observability of 2D SLAM-JSBE. Following this methodology, an observability analysis of single landmark SLAM-JSBE shows that the observability matrix \mathbf{G}_O of the system is rank deficient by 4. A rank analysis of the observability matrix, with increasing number of unknown landmarks in the state vector, further establishes that the rank deficiency remains 4. However, it is interesting to note that the observability matrix of 2D SLAM-JSBE becomes full rank when observations from at least two a priori known landmarks are incorporated into the observation model in addition to the observations of all the unknown landmarks, which are being estimated. A necessary condition for full observability of 2D MAL-JSBE [15] and SLAM-JSBE is that at least two known landmarks must be observed at all times. However there can still be conditions that prevent the system from achieving full observability depending on the robot trajectory and the relative configuration of the observed known and unknown landmarks as is given in Result 5.

Result 5: If the two observed known landmarks are collinear with the vehicle then 2D SLAM-JSBE becomes unobservable.

Result 6: The necessary conditions for full observability of IMU aided SLAM-JSBE involving any numbers of unknown 2D landmarks are satisfied if the non-holonomic constraints are imposed, all the unknown landmarks are observed and at least two known 2D landmarks are observed simultaneously (see Section IVB).

IV. APPLICATION - BIAS CORRECTION IN IMU AIDED SLAM

A. Problem Formulation

Some of the major shortcomings of inertial measurement units (IMUs) are their inherent sensor biases, drifts and scale factors, which adversely affect the accuracy of any position estimate ([18] and [20]). It is therefore important that the effects of sensor biases on inertial sensor (proprioceptive sensor) aided SLAM are investigated. A vehicle (Fig. 1) is assumed to move in an environment consisting of static landmarks. An inertial sensor assembly is mounted at the centre of gravity (COG) of the vehicle. The landmark positions are represented by their lateral and longitudinal (x, y) coordinates. The vehicle body reference frame $\{\mathbf{v}\}$ with origin at the COG of the vehicle coincides with the inertial measurement unit's (IMU) coordinate frame. The vehicle frame, $\{\mathbf{v}\}$'s X-axis is pointing along the heading direction and the other orthogonal axes Y-axis and

Z-axis are shown in the Fig. 2. The orientation of the vehicle body frame $\{\mathbf{v}\}$ is represented by the three Euler angles ϕ (rotation about vehicle X axis or roll), θ (rotation about vehicle Y axis or pitch) and ψ (rotation about vehicle Z axis or yaw) also shown in Fig. 2. The vehicle motion is referred to a global frame, which is the navigation frame $\{\mathbf{n}\}$ with its orthogonal axes pointing to North, East and Down (ENU). Let the vehicle state vector $\mathbf{x}_v(k)$ at time k be

$$\mathbf{x}_v(k) = [\underline{\mathbf{x}}^n \ \underline{\mathbf{v}}^n \ \phi \ \theta \ \psi \ \mathbf{x}_b]^T \quad (18)$$

where $\underline{\mathbf{x}}^n = [x_v^n \ y_v^n \ z_v^n]^T$, $\underline{\mathbf{v}}^n = [v_x^n \ v_y^n \ v_z^n]^T$ and $x_v^n, y_v^n, z_v^n, v_x^n, v_y^n$ and v_z^n are position coordinates and velocities of the vehicle along X axis, Y axis and Z axis respectively all with reference to the fixed navigation frame $\{\mathbf{n}\}$. The concatenated bias vector \mathbf{x}_b at time k is given by

$$\mathbf{x}_b(k) = [b_{xa}^v \ b_{ya}^v \ b_{za}^v \ b_{x\omega}^v \ b_{y\omega}^v \ b_{z\omega}^v]^T \quad (19)$$

where $b_{xa}^v, b_{ya}^v, b_{za}^v, b_{x\omega}^v, b_{y\omega}^v$ and $b_{z\omega}^v$ are the biases in the IMU acceleration and angular rate measurements along and about the vehicle X, Y and Z axes respectively.

As discussed in the previous sections of this paper as well as in [10] and [12], the biases associated with the inertial sensors are appropriately modeled using constant terms and a random walk processes (this can accommodate the exponential variation of biases [10] as well) as follows.

$$\mathbf{x}_b(k) = \mathbf{A}_b \mathbf{x}_b(k-1) + \mathbf{c}_b^v + \boldsymbol{\eta}_b^v \quad (20)$$

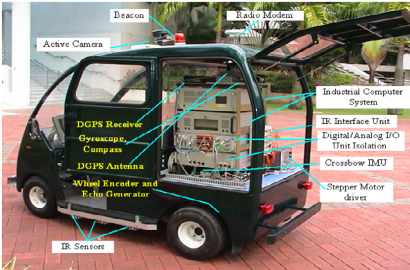


Fig. 1. Mobile robot used in SLAM experiments

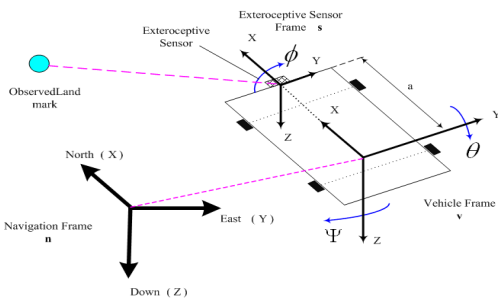


Fig. 2 Reference coordinate frames in inertial sensor aided SLAM

where \mathbf{A}_b is a 6×6 diagonal matrix, \mathbf{c}_b^v is a 6×1 constant vector and $\boldsymbol{\eta}_b^v$ is a 6×1 temporally uncorrelated noise vector having the diagonal covariance matrix \mathbf{Q}_b . The values of \mathbf{A}_b , \mathbf{c}_b^v and \mathbf{Q}_b can be experimentally

determined as in [12].

The inertial sensor aided SLAM with bias estimation problem has a composite state vector $\mathbf{X}(k)$

$$\mathbf{X}(k) = [\mathbf{x}_v^T(k) \ \mathbf{m}^T(k)] \quad (21)$$

where $\mathbf{m}(k) = \mathbf{m}(k-1)$ and $\mathbf{x}_v(k)$ evolves as discussed in [15] for IMU aided localization with a known map.

It is assumed that the vehicle moves on a flat surface thus constraining z_v^n to a constant value. Landmarks are assumed to be observed using an onboard exteroceptive sensor such as a 2D scanning range-bearing sensor.

As shown in Fig. 2, the vehicle body fixed exteroceptive sensor frame $\{\mathbf{s}\}$ is assumed to be aligned, but not coincident, with the vehicle frame $\{\mathbf{v}\}$. Let \mathbf{x}_s^v represent the position of the exteroceptive sensor in $\{\mathbf{v}\}$, \mathbf{x}_s^n the position of the exteroceptive sensor in $\{\mathbf{n}\}$, \mathbf{x}_m^n the coordinates of a point landmark in $\{\mathbf{n}\}$, and $\mathbf{x}_m^s = [m_x \ m_y \ m_z]^T$ its coordinates in the exteroceptive sensor's frame $\{\mathbf{s}\}$. Since the vehicle moves on a horizontal plane with known elevation, the z coordinates of the position vectors \mathbf{x}_s^v , \mathbf{x}_s^n , \mathbf{x}_m^n , and \mathbf{x}_m^s are fixed and known a priori. Since \mathbf{C}_{vn} is the relative orientation between $\{\mathbf{v}\}$ and $\{\mathbf{n}\}$, we have

$$\mathbf{x}_s^n = \mathbf{x}_s^v + \mathbf{C}_{vn} \mathbf{x}_m^s, \ \mathbf{x}_m^s = (\mathbf{C}_{vn})^T (\mathbf{x}_m^n - \mathbf{x}_s^n) \quad (22)$$

$$\mathbf{z}(k) = \left[\sqrt{m_x^2 + m_y^2} \ \tan^{-1}(m_y/m_x) + \pi/2 \right]^T \quad (23)$$

Since the vehicle motion is constrained by the nonholonomic constraints, (i.e. vehicle velocities along the Y-axis v_y^v and Z-axis v_z^v of the vehicle reference frame $\{\mathbf{v}\}$ are zero) we use these constraints [11] as additional (virtual) observations in the online bias estimation. Let the x component of the vehicle velocity be v_x^v , then

$$[v_x^v \ v_y^v \ v_z^v]^T = (\mathbf{C}_{vn})^T [v_x^n \ v_y^n \ v_z^n]^T \quad (24)$$

$$v_y^v = 0 + \eta_x \quad (25)$$

$$v_z^v = 0 + \eta_z \quad (26)$$

where η_x and η_z are Gaussian noise sequences representing the amount of constraint violation [31].

B. Maintaining Observability in IMU Aided SLAM-JSBE

Through symbolic manipulation of the vehicle motion and observations models ((18)-(26)) in accordance with the theory detailed in Section IID, the necessary conditions for the observability of the inertial sensor aided SLAM-JSBE can be derived (see Result 6).

C. Experiments

The in-house built mobile robot (Fig. 1) was used in the SLAM-JSBE experiments described here. An un-calibrated IMU (Crossbow DMU-AHRS) was mounted at the COG of the mobile robot as shown in Fig. 2. The mobile robot was driven at approximately 4m/s in a car park where the surface was relatively flat and horizontal. A SICK LMS 290 scanning range/bearing measurement sensor, mounted as

shown in Fig. 2, was used as the exteroceptive sensor. The IMU and LMS range scans were sampled at 100 Hz and 10Hz respectively.

Feature extraction was achieved using a simple clustering strategy based on the distance between contiguous and adjacent range points. In this experiment the locations of a few prominent landmarks were hand measured and taken as known landmarks. Artificial fiber glass poles were also used as the known landmarks. These were selected so that at least two or more of them are always visible to the LMS exteroceptive sensor. Figs. 3 and 4 show the variation of the biases and Figs. 5 and 6 the variation of the 95% confidence bounds of the uncertainties of the estimated biases. Figs. 3 – 6 show the results of estimation of the biases in accelerometers and gyroscopes. In order to evaluate the estimated results initial systematic and associated noise components of the IMU biases were estimated offline as described in [12] using data obtained when the vehicle was stationary. On average, these off-line estimates of the initial bias components in the x, y and z directions of the accelerometers were 0.075 ms^{-2} , 0.08 ms^{-2} , and 0.08 ms^{-2} respectively, and in the gyroscopes, 0.02 rad/s in all three directions. It may be noted that the initial estimated sensor bias components (Figs 3-6) are close to the values obtained by the offline algorithm described in [12]. Fig. 7 illustrates the estimated vehicle path and landmarks. DGPS measurements obtained at 1 Hz is also plotted along the vehicle trajectory to compare the “true” (obtained through GPS) and the estimated trajectories. Fig. 8 shows the estimated landmarks and their 95% confidence limits of uncertainties. The results of Fig. 8 verify that the landmark estimation errors are bounded by their 95% confidence limits.

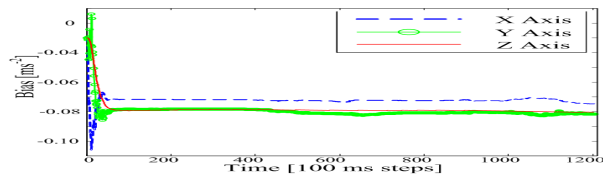


Fig. 3 Estimation of accelerometer biases

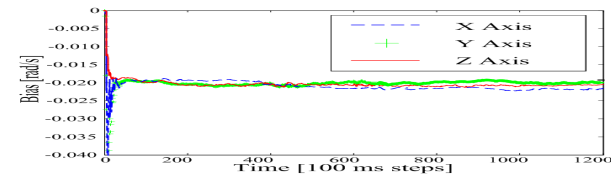


Fig. 4 Estimation of gyroscope biases

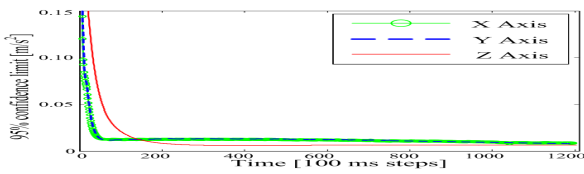


Fig. 5 Estimation of 95% confidence limits of accelerometer biases

Figs. 9-10 show the estimated landmark positions against the measured ground truth of the static landmarks. The ground truth of the landmarks was obtained by hand measurements. It may be noted that the “true errors” in the landmark estimates are well within the 95% confidence

bounds implying the consistency of the filter. However, it is of interest to note in Figs. 9 – 10 that the landmark x and y position estimation errors seem to exhibit a deterministic trend. This is a consequence of the non-satisfaction of the full observability condition for that particular landmark at all times. To guarantee full observability it is necessary that the landmark is observed by the exteroceptive sensor (LMS291) at all times.

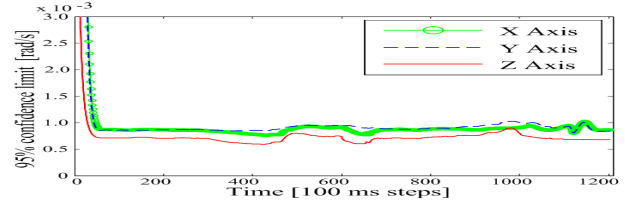


Fig. 6 Estimation of 95% confidence limits of gyroscope biases

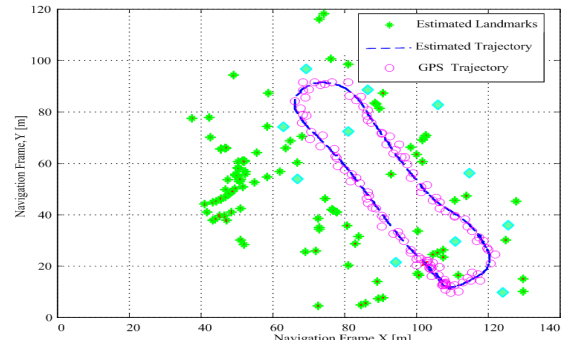


Fig. 7 Estimated robot trajectory and landmark locations. Known landmarks are indicated by diamond shaped markers

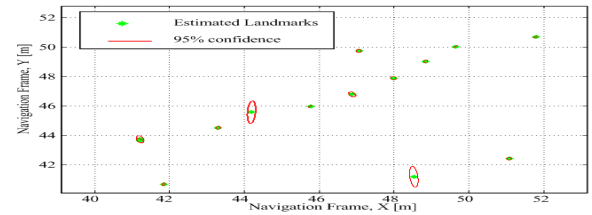


Fig. 8 Estimation of landmark uncertainties.

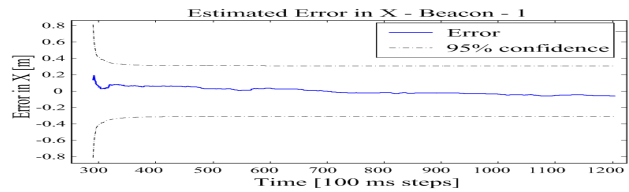


Fig. 9 Estimation of the longitudinal error of landmark 1.

Nevertheless, as proven and discussed in Section IV B, the results of the experiment verify that given sufficient number of known landmark observations the biases of the accelerometers and rotational rate sensors (proprioceptive sensors) of the inertial sensor aided SLAM-JSBE can be estimated online.

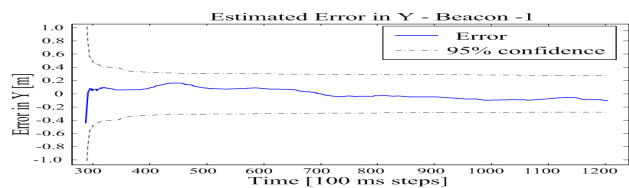


Fig. 10 Estimation of the lateral error of landmark 1.

V. CONCLUSIONS

Biases in both proprioceptive and exteroceptive sensors can adversely impact the performance of EKF-SLAM. However, through explicit modeling of biases in sensors and their incorporation in the standard EKF-SLAM formulation it is possible to on-line estimate them and hence improve performance. In addition several important properties of this complex joint estimation filter are theoretically established for simple 1D EKF-SLAM and more realistic 2D EKF-SLAM scenarios and experimentally verified for the latter. The contributions thus made in each case can be summarized as follows. Although the angle between controllable and observable subspaces in 1D EKF-SLAM approaches zero when the number of observed landmarks are made infinitely large, it is not so in 1D EKF-SLAM-JSBE. The problem is fully observable if the vehicle's absolute position measurement and the range measurement of a known landmark is incorporated into the observation vector comprising of all the measurements of all the unknown estimated landmarks.

The rate of convergence of the filter is affected by the relative strengths of noises of the proprioceptive and exteroceptive sensors and the number of landmarks observed. More specifically, the smaller the ratio between the exteroceptive sensor noise and the process noise (proprioceptive sensor noise and the modeling uncertainty) or, the larger the number of landmarks observed simultaneously (either known landmarks or the estimated landmarks or both), the faster will be the convergence of the state variances to their steady state values.

In the more realistic scenario involving 2D SLAM-JSBE, the uncertainties in the estimates of the proprioceptive and exteroceptive sensor bias parameters diminish monotonically in an update of the SLAM algorithm. The errors in the exteroceptive sensor biases reach a certain lower bound as determined by the process and observation model accuracies. The necessary condition for the observability of the 2D SLAM-JSBE problem is satisfied when observations from two or more a priori known landmarks are incorporated in the observation model in addition to the observations of all the unknown landmarks, being estimated.

However, if any two of these known landmarks are collinear with the vehicle the problem becomes unobservable. In the case of IMU aided SLAM-JSBE, full observability is satisfied if non-holonomic constraints are imposed, all estimated landmarks are observed together with at least two known landmarks. The SLAM-JSBE problem formulation, the theoretical results established and experimental results provide greater insight into the problems of estimation theoretic bias correction in MAL and SLAM paving the way for improved design of process and observation models and also the selection of appropriate sensors for the enhanced performance of localization and mapping algorithms depending on the requirements of the mobile robot application.

APPENDIX

Proof of Result 1:

Image(\mathbf{G}_o^T) and Image(\mathbf{G}_c) consists of $n+1$ and 1 basis vectors respectively. Let $\underline{\mathbf{r}}_i$, for $i=1,2,\dots,n+1$ be the basis

vectors of Image(\mathbf{G}_o^T) and $\underline{\mathbf{q}}$ be the basis vector of Image(\mathbf{G}_c). Suppose $\underline{\mathbf{p}}$ be the projection of the basis of Image(\mathbf{G}_c) into the basis spanned by Image(\mathbf{G}_o^T). Thus, using the algebra of vector transformations and projections:

$$\underline{\mathbf{p}} = \sum_{i=1}^{n+1} \frac{\underline{\mathbf{q}}^T \underline{\mathbf{r}}_i}{\underline{\mathbf{r}}_i^T \underline{\mathbf{r}}_i} \underline{\mathbf{r}}_i = \sum_{i=1}^n \frac{\underline{\mathbf{q}}^T \underline{\mathbf{r}}_i}{\underline{\mathbf{r}}_i^T \underline{\mathbf{r}}_i} \underline{\mathbf{r}}_i + \frac{\underline{\mathbf{q}}^T \underline{\mathbf{r}}_{n+1}}{\underline{\mathbf{r}}_{n+1}^T \underline{\mathbf{r}}_{n+1}} \underline{\mathbf{r}}_{n+1},$$

Since $\underline{\mathbf{q}}^T \underline{\mathbf{r}}_{n+1} = 0$, $\underline{\mathbf{r}}_i^T \underline{\mathbf{r}}_i = 3$ for all i and $\underline{\mathbf{p}}^T \underline{\mathbf{q}} = n/3$.

$$\psi = \cos^{-1} \left(\frac{(\underline{\mathbf{p}}^T \underline{\mathbf{q}})}{(\|\underline{\mathbf{p}}\| \|\underline{\mathbf{q}}\|)} \right) = \cos^{-1} \left(\frac{n}{\sqrt{n(2n+1)}} \right).$$

Proof of Result 3:

By expanding the error covariance matrix $\mathbf{P}(k|k-1)$ of $\mathbf{X}(k)$ of the model given by (15)-(17) we can deduce the covariance predictions of the sensor biases as follows.

$$\mathbf{P}_{uu}(k|k-1) = \mathbf{P}_{uu}(k-1|k-1) \quad (27)$$

$$\mathbf{P}_{ss}(k|k-1) = \mathbf{P}_{ss}(k-1|k-1) \quad (28)$$

$\mathbf{P}(0|0)$, $\mathbf{Q}(k)$ and $\mathbf{R}(k)$ are positive semi definite (PSD) matrices. Thus, by using the properties (see [7]) of PSD matrices, $\mathbf{S}(k)$ and $\mathbf{K}(k)\mathbf{S}(k)\mathbf{K}^T(k)$ can also shown to be PSD matrices. Hence

$$\det(\mathbf{P}(k|k)) = \det(\mathbf{P}(k|k-1) - \mathbf{K}(k)\mathbf{S}(k)\mathbf{K}^T(k)) \quad (29)$$

$$\det(\mathbf{P}(k|k)) \leq \det(\mathbf{P}(k|k-1)) \quad (30)$$

Since any principal submatrix of a PSD matrix is also PSD;

$$\det(\mathbf{P}_{uu}(k|k)) \leq \det(\mathbf{P}_{uu}(k|k-1)) \quad (31)$$

$$\det(\mathbf{P}_{ss}(k|k)) \leq \det(\mathbf{P}_{ss}(k|k-1)) \quad (32)$$

Therefore from (31) and (32),

$$\det(\mathbf{P}_{uu}(k|k)) \leq \det(\mathbf{P}_{uu}(k-1|k-1)) \quad (33)$$

$$\det(\mathbf{P}_{ss}(k|k)) \leq \det(\mathbf{P}_{ss}(k-1|k-1)) \quad (34)$$

The determinants of the covariance matrices indicate the volume or size of their uncertainty ellipsi and therefore it can be concluded that the errors in the estimates of the bias parameters diminish in a measurement update of the SLAM algorithm. This rationale is also true for the uncertainties of the sensor biases of 2D MAL-JSBE, as shown in the results in [15].

Proof of Result 4:

It may be noted that the lowest exteroceptive sensor bias covariance estimates are obtained when the proprioceptive sensor noise covariance and the modeling uncertainty (process noise covariance \mathbf{Q}) and the observation noise covariance (\mathbf{R}) are minimum. For example when the vehicle is stationary ($\mathbf{Q} = \mathbf{0}$) whilst observing an unknown landmark we have such a scenario. Under such a scenario the composite SLAM state vector is

$$\mathbf{X}(k) = \begin{bmatrix} \mathbf{x}_v^T(k) & \mathbf{m}^T(k) & \mathbf{s}_b^T(k) \end{bmatrix}^T \quad (35)$$

where the map $\mathbf{m}(k)$ consists of the unknown landmark location vector, which has to be estimated. The observation model is $\mathbf{H}(k) = \begin{bmatrix} -\mathbf{H}_v(k) & \mathbf{H}_m(k) & \mathbf{I}_{ss} \end{bmatrix}$ where $-\mathbf{H}_v(k)$ and

$\mathbf{H}_m(k)$ denote the parts of the observation matrix corresponding to the vehicle state and the landmark state respectively. Since $\mathbf{Q} = \mathbf{0}$ the predicted covariance matrix $\mathbf{P}(k | k-1)$ for all k is,

$$\mathbf{P}(k | k-1) = \mathbf{P}(k-1 | k-1) \quad (36)$$

Using the inverse covariance form ([8]),

$$\mathbf{P}^{-1}(k | k) = \mathbf{P}^{-1}(k | k-1) + \mathbf{H}^T(k) \mathbf{R}^{-1}(k) \mathbf{H}(k) \quad (37)$$

Hence, when making k observations

$$\mathbf{P}^{-1}(k | k) = (\text{diag}(\mathbf{P}_v, \mathbf{P}_m, \mathbf{P}_s))^{-1} + k \mathbf{H}^T(k) \mathbf{R}^{-1}(k) \mathbf{H}(k).$$

Thus, omitting the notation for time index k (eg. $\mathbf{H} = \mathbf{H}(k)$) and using $\text{diag}(\mathbf{P}_v, \mathbf{P}_m, \mathbf{P}_s)$ as the initial covariance matrix of $\mathbf{X}(k)$, the exteroceptive sensor bias covariance matrix, $\mathbf{P}_{ss}(k | k)$ can be determined as;

$$\mathbf{P}_{ss} = ((\mathbf{P}_s^{-1} + k \mathbf{R}^{-1}) + k \mathbf{R}^{-1} \mathbf{H}_v (-\mathbf{a}_{11} \mathbf{H}_v^T \mathbf{R}^{-1} + \mathbf{a}_{12} k \mathbf{H}_m^T \mathbf{R}^{-1}) - k \mathbf{R}^{-1} \mathbf{H}_m (-\mathbf{a}_{21} \mathbf{H}_v^T \mathbf{R}^{-1} + \mathbf{a}_{22} k \mathbf{H}_m^T \mathbf{R}^{-1}))^{-1} \quad (38)$$

Since zero vehicle and proprioceptive sensor uncertainties were assumed in the above derivation, the inverse of \mathbf{P}_{ss} represents the maximum information one can gain on $\mathbf{s}_b(k)$. Subsequently as information from more observations are obtained, the upper limit of this information gain will be reached (if at all a limit exists). Conversely, if this finite limit exists, the covariance of the exteroceptive sensor bias term \mathbf{P}_{ss} will be lower bounded by \mathbf{P}_{ss}^* .

$$\mathbf{P}_{ss}^* = \lim_{k \rightarrow \infty} (\mathbf{P}_{ss}) \quad (39)$$

Proof of Result 5:

Assume that the exteroceptive sensor observes two known landmarks denoted by $\mathbf{LM}_1 \equiv (x_1, y_1)$ and $\mathbf{LM}_2 \equiv (x_2, y_2)$ and an unknown landmark $\mathbf{LM}_3 \equiv (x_3, y_3)$. Assuming that the point of the vehicle that is being estimated and the exteroceptive sensor location coincide, the measurement Jacobian \mathbf{H} when observing all three landmarks simultaneously is

$$\mathbf{H} = \begin{bmatrix} \mathbf{H}\mathbf{V}_3 & \mathbf{0}_2 & \mathbf{I}_2 & \mathbf{H}\mathbf{L}_3 \\ \mathbf{H}\mathbf{V}_1 & \mathbf{0}_2 & \mathbf{I}_2 & \mathbf{0}_2 \\ \mathbf{H}\mathbf{V}_2 & \mathbf{0}_2 & \mathbf{I}_2 & \mathbf{0}_2 \end{bmatrix} \quad (40)$$

where $\mathbf{H}\mathbf{V}_i = \begin{bmatrix} \Delta x_i / \Delta r_i & \Delta y_i / \Delta r_i & 0 \\ -\Delta y_i / (\Delta r_i)^2 & \Delta x_i / (\Delta r_i)^2 & -1 \end{bmatrix}$ for all

$$i = 1, 2, 3 \quad \mathbf{H}\mathbf{L}_3 = \begin{bmatrix} -\Delta x_3 / \Delta r_3 & -\Delta y_3 / \Delta r_3 \\ \Delta y_3 / (\Delta r_3)^2 & -\Delta x_3 / (\Delta r_3)^2 \end{bmatrix},$$

$\Delta x_i = x(k | k-1) - x_i$, $\Delta y_i = y(k | k-1) - y_i$ and $\Delta r_i = \sqrt{(\Delta x_i)^2 + (\Delta y_i)^2}$ for all $i = 1, 2, 3$ When the two known landmarks being observed and the vehicle are collinear,

$$\Delta x_1 / \Delta x_2 = \Delta y_1 / \Delta y_2 = \Delta r_1 / \Delta r_2 \quad (41)$$

When (41) is true, the matrix \mathbf{H} has linearly dependent rows. Under such circumstances, the observability matrix becomes rank deficient. Hence one of the necessary conditions for full observability of SLAM-JSBE is violated.

REFERENCES

- [1] L.D.L.Perera, W.S. Wijesoma, S. Challa, M.D.Adams, "Sensor Bias Correction in Simultaneous Localization and Mapping", International Conference of Information Fusion, Cairns, Australia, July 2003, pp 151-158.
- [2] S.P. Dmtriev, O.A. Stepanov and S.V. Shepel, "Nonlinear Filtering Methods Application in INS Alignment", IEEE Transactions on Aerospace and Electronic Systems, Vol. 33, No.1, January 1997, pp. 260-272.
- [3] M.B. Igngni, Optimal and Suboptimal Separate Bias Kalman Estimators for a Stochastic Bias, IEEE Transactions on Automatic Control, Vol 45-3, 2000, pp 547-551.
- [4] M.W.M.G. Dissanayake, P. Newman, S. Cleark, H.F. Durrant-Whyte and M. Csorba, "A Solution to the Simultaneous Localization and Map Building (SLAM) Problem", IEEE Transactions on Robotics and Automation, Vol 17, No 3, pp 229-241, June 2001.
- [5] Y. Bar-Shalom, "Mobile Radar Bias Estimation Using Unknown Location Targets", Proceedings of the 3rd International Conference on Information Fusion, Paris, France, July 2000, pp TuC1-3 – TuC1-6.
- [6] N. Okelleo, S. Challa, "Joint sensor registration and track to track fusion for distributed trackers", Internal Technical Report, Cooperative Research Centre for Sensor Signal and Information Processing, Department of electrical and electronic engineering, University of Melbourne, Australia, January 2003.
- [7] R. A. Horn, C.R. Johnson, "Matrix Analysis", Cambridge University Press, 1985.
- [8] Yaakov Bar-Shalom, X. R. Li, "Estimation with Applications to Tracking and Navigation: Theory Algorithms and Software", John Wiley and Sons, Inc., 2001.
- [9] K. Reif, S. Gunther, E. Yaz, R Unbehauen, "Stochastic Stability of the Discrete-Time Extended Kalman Filter", IEEE Transactions on Automatic Control, Vol 44, No.4, pp714-278, April 1999.
- [10] M.G. Grewal, L.R. Weill, A.P. Andrews, "Global Positioning Systems, Inertial Navigation and Integration", John Wiley and Sons Inc. New York, 2001.
- [11] M. Koifman and Y. Bar-Itzhack, "Inertial Navigation Systems Aided by Aircraft Dynamics.", IEEE Transactions on Control Systems Technology, Vol 7, pp 487-497, July 1999.
- [12] E. Nebot and H. Durrant-Whyte, "Initial Calibration and Alignment of Low-Cost Inertial Navigation Units for Land Vehicle Applications", Journal of Robotic Systems, Vol. 16, No.2, 1999, pp. 81-92. [[21
- [13] S. Hong, M. H. Lee, S. H. Kwon and H. H. Chun, "A Car Test for the Estimation of GPS/INS Alignment Errors", IEEE Transactions On Intelligent Transportation Systems, VOL. 5, NO. 3, SEPTEMBER 2004, pp. 208-218.
- [14] B. Southall, B.F. Buxton and J.A. Marchant, "Controllability and Observability: Tools for Kalman Filter Design", Proceedings. of British Machine Vision Conference BMVC 1998, vol. 1, pp. 164-173, 1998.
- [15] L. D. L. Perera, W. S. Wijesoma, and M. D. Adams, "The estimation theoretic sensor bias correction problem in map aided localization", *International Journal of Robotics Research*, vol. 25, No. 7, pp 645-667, July 2006.
- [16] P.W. Gibbens, M.W.M.G. Dissanayeke and H.F. Durrant-Whyte, "A Closed Form Solution to the Single Degree of Freedom Simultaneous Localization and Map Building (SLAM) Problem", Proceedings. of IEEE International Conference on Decision and Control, vol. 39, pp. 191-196, 2000.
- [17] J. Andrade-Cetto and A. Sanfeliu, "The Effects of Partial Observability When Building Fully Correlated Maps", IEEE Transactions on Robotics, Vol 21, No. 4, pp 771-777, August 2005.
- [18] M.G. Grewal, L.R. Weill, A.P. Andrews, "Global Positioning Systems, Inertial Navigation and Integration", John Wiley and Sons Inc. New York, 2001.
- [19] D. Fox, W. Burgard, F. Dellart and S. Thrun, "Monte Carlo Localization: Efficient Position Estimation for Mobile Robots", Proceedings of the 16th National Conference on Artificial Intelligence (AAAI 99), 1999.
- [20] L. Bingbing and M.D. Adams, "Multi Aided Inertial Navigation for Ground Vehicles in Outdoor Uneven Environments", Proceedings of the IEEE International Conference on Robotics and Automation, Barcelona, Spain, 2005.